Vertical emitting aperture nanoantennas

Ami Yaacobi,* Erman Timurdogan, and Michael R. Watts

Photonic Microsystems Group, Research Laboratory of Electronics, Massachusetts Institute of Technology, 77 Massachusetts Avenue, Cambridge, Massachusetts 02139, USA

**Corresponding author: amiya@mit.edu*

Received November 4, 2011; revised March 1, 2012; accepted March 8, 2012; posted March 12, 2012 (Doc. ID 157627); published April 24, 2012

Herein we propose, theoretically investigate, and numerically demonstrate a compact design for a vertical emitter at a wavelength of 1.5 μm based on nanophotonic aperture antennas coupled to a dielectric waveguide. The structure utilizes a plasmonic antenna placed above a Si_3N_4 waveguide with a ground plane for breaking the up—down symmetry and increasing the emission efficiency. Three-dimensional (3-D) finite-difference time-domain (FDTD) simulations reveal that up to 60% vertical emission efficiency is possible in a structure only four wavelengths long with a 3 dB bandwidth of over 300 nm.

OCIS codes: 250.5403, 130.0130.

Vertical input/output coupling in the telecom C-band (i.e., 1535 nm $< \lambda <$ 1565 nm) has been extensively investigated for the purpose of coupling to or from an optical fiber [1–4]. As a result, most vertical couplers to date have emission patterns matched to fiber modal diameters (~10 μm). However, vertical coupling can also be used in optical phased arrays [5,6] to steer a beam or generate holograms. In a phased array, the desired emitter characteristics include strong waveguide-to-free-space output coupling and a compact structure (i.e., a few wavelengths long or less). A short emitter length is critical to fitting many emitters in a small area and enabling wide rotation angles with a single lobe. However, demonstrations of efficient output coupling using short structures are uncommon with minimum structure lengths of several wavelengths [2,4]. Most vertical couplers (with the exception of the metallic rods in [7,8]) rely on gratings in semiconductors or insulators alone to perturb the electromagnetic field and efficiently emit. However, the extraction rate is limited by index contrasts available in dielectric structures. To overcome this limitation, we consider the use of metals to perturb the electromagnetic field and achieve efficient vertical coupling in a compact structure. We show that the inherent large permittivities and conductivities of metals enable large coupling coefficients and efficient output in a structure only a few wavelengths long. The specific structure designed here is a nanophotonic aperture antenna. However, the results here are general; designed properly, nanoantennas enable rapid emission from dielectric waveguides.

To gain intuition about the coupling between the nanoantenna and the waveguide, we treat the nanoantenna as a resonator using coupled-mode theory in the time domain [9,10]. While coupled-mode theory assumes shape invariance of the modes and drops second order terms making it more quantitatively accurate with weakly coupled modes, coupled mode theory provides useful insight even when modes are strongly coupled. However, for quantitatively accurate results, in this letter, we rely on three-dimensional (3-D) full field simulations.

The differential equation governing the response of a resonator with energy amplitude a and coupling coefficient μ to a perturbing mechanism (e.g., a waveguide) with wave amplitude s (normalized to power) is, to first order,

$$\frac{da}{dt} = \left(j\omega_0 - \frac{1}{\tau}\right)a + \mu s, \tag{1}$$

where ω_0 is the resonant frequency, and τ is its decay rate. In a nanophotonic antenna, the loss mechanisms can be broken down into radiation, ohmic, and coupling losses, with decay rates τ_r, τ_o, and τ_e, respectively. From energy balance considerations, we have

$$\frac{1}{\tau} = \frac{1}{\tau_e} + \frac{1}{\tau_r} + \frac{1}{\tau_o}, \tag{2}$$

where the waveguide coupling τ_e is considered in both waveguide directions. The steady state solution to Eq. (1) with ω frequency input s is

$$a = \frac{\mu s}{j(\omega - \omega_0) + 1/\tau}. \tag{3}$$

From energy balance considerations, μ is related to τ_e through $|\mu|^2 = 2/\tau_e$ [Eq. (6) in 10]. Given that our goal is to maximize the ratio of the radiated power $|s_r|^2 = 2|a|^2/\tau_r$ [Eq. (7) in 10] to incident power $|s|^2$, and assuming that τ_r remains constant, we substitute $\mu = (2/\tau_e)^{1/2}$ and τ from Eq. (2) into (3). We then maximize $|a/s|$ with $\omega = \omega_0$ and find the desired value of τ_e to be $\tau_e = \tau_r$ when ohmic losses are neglected.

The effect of changes to our structure on τ_e or μ can be estimated using coupled-mode theory. This section follows the formalism developed in [11] for time dependent coupling using volume integration and is therefore consistent with 3-D modes. Following Eqs. 2.13 to 2.16 in [11], we look at the power fed by the waveguide to the resonator mode

$$-\frac{1}{2}\,\mathrm{Re}\int \mathbf{E}^* \cdot \mathbf{J}\mathrm{d}V = -\frac{1}{4}\int (a\mathbf{e}_\mathrm{r})^* \cdot (j\omega\Delta\varepsilon s\mathbf{e}_\mathrm{wg})\mathrm{d}V + c.c., \tag{4}$$

where $\mathbf{e}_\mathrm{r}$ and $\mathbf{e}_\mathrm{wg}$ are the normalized modes of the resonator and waveguide, respectively. $\mathbf{J} = j\omega\mathbf{P} = j\omega\Delta\varepsilon s\mathbf{e}_\mathrm{wg}$ is the polarization current due to the perturbation from the resonator and $\Delta\varepsilon$ is the complex permittivity difference caused by the resonator. Looking at the energy change in the resonator

$$\frac{\mathrm{d}|a|^2}{\mathrm{d}t} = \frac{-2}{\tau}aa^* + \mu a^* s + \mu^* a s^*, \tag{5}$$

the power from (4) corresponds to the last two terms only ($\mu a^* s + \mu^* a s^*$). Thus, μ is given by

$$\mu = \frac{-j}{4}\omega \int \Delta\varepsilon \mathbf{e}_r^* \cdot \mathbf{e}_{\mathrm{wg}} \mathrm{d}v. \tag{6}$$

In the formulation above, we define the waveguide three dimensional mode as $\mathbf{e}_{\mathrm{wg}} = \tilde{\mathbf{e}}_{\mathrm{wg}}(x, y)\exp(-j\beta z)$ where $\tilde{\mathbf{e}}_{\mathrm{wg}}$ is the two dimensional waveguide mode. Equation (6) shows that the high absolute value of $\Delta\varepsilon$ for a metallic perturbation increases the polarization current and hence, gives rise to efficient coupling in a small volume.

Vertical coupler designs in this paper are based on rectangular apertures in an antenna plane placed above a Si_3N_4 waveguide, with an additional metallic ground-plane under that waveguide to facilitate vertical coupling [Fig. 1]. As an example realistic structure, we chose the following: (1) an 80 nm Al ground-plane, (2) a 60 nm Al antenna layer, (3) a Si_3N_4 waveguide with a width of 700 nm and a 220 nm height, (4) a ground plane to antenna separation of 680 nm, and (5) a waveguide to antenna separation of 100 nm [Fig. 1(a)]. The permittivities of Si_3N_4 and SiO_2, are 4 and 2.1, respectively at 1550 nm [12], and the Al Drude parameters are $\gamma_d = 2.4 \times 10^{14}$ rad/sec and $\omega_p = 2.2 \times 10^{16}$ rad/sec.

In order to calculate τ_e and τ_r, we look at the ring-down properties of the resonator. When no input excitation is applied ($s = 0$) the solution for (1) is the exponential ring-down

$$a(t) = a(0)\exp(j\omega_0 t - t/\tau). \tag{7}$$

3-D finite-difference time-domain (FDTD) ring-down simulations of just the antenna in Fig. 1 (without the Si_3N_4 waveguide) give us the radiation rate τ_r of the antenna. Fig. 2 shows the ring-down of a single rectangular aperture resonator, tuned to a resonance near 1550 nm, when it is isolated and also when coupled to a waveguide. The resulting τ_r (neglecting ohmic losses) is found to be ~7 fs when no waveguide is present. The combined time

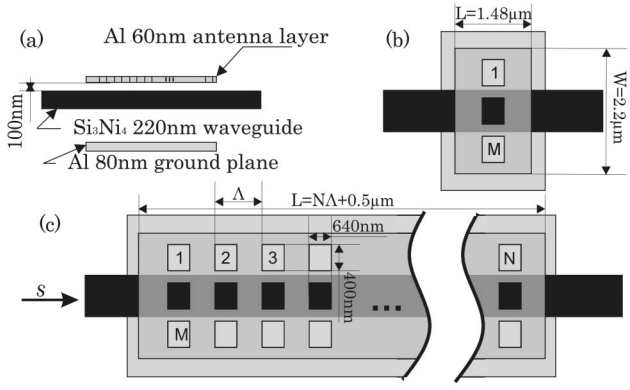

Fig. 1. Antenna designs. (a) Side view. (b) Top view of laterally repeating apertures. (c) Longitudinally repeating with period $\Lambda = 0.9\ \mu\mathrm{m} < \lambda/n$. The underlayer of Al represents a ground plane positioned at $d = 3\lambda/4n$ (680 nm) from the emitter metal.

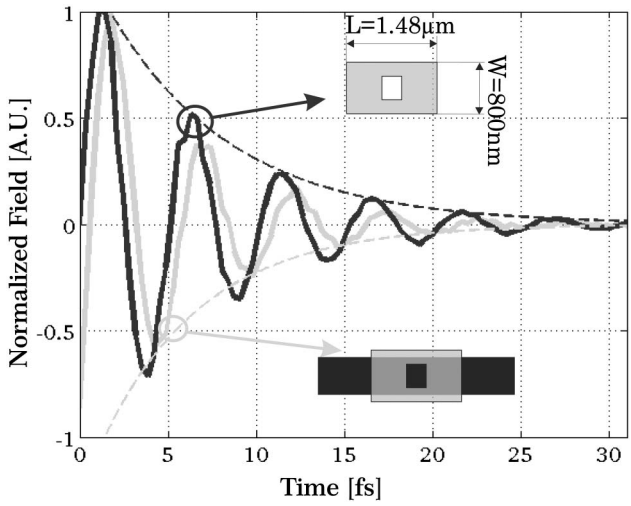

Fig. 2. 3-D FDTD ring-down simulation of the electric field (and its exponential envelope) for a single aperture resonator without (black) and with (gray) a waveguide. The fields (i.e., lateral electric fields) were taken from the aperture center.

constant for radiation plus waveguide coupling, τ, is found to be about 5.8 fs. Using Eq. (2), the external coupling coefficient is found to be $\tau_e \approx 34$ fs, five times larger than the radiation coupling τ_r. Although the result above is approximate, as τ_r can vary with the introduction of the waveguide, the fact that τ_e is much greater than τ_r indicates that the resonator is clearly under-coupled.

To increase the coupling to the resonator, one can, for example, lower the metal level to bring the antenna closer to the feeding waveguide or reshape the antenna's input side (e.g., using a metal-insulator-metal feeder to the aperture). Our approach was to coherently repeat the antenna aperture and, by doing so, increase the waveguide to resonator coupling coefficient μ [Fig. 1(b)].

From Eq. (6), it becomes clear that repeating the antenna structure laterally will preferentially increase the overlap integral to the lowest order mode by the adding volume with non-zero $\Delta\varepsilon$. Taking into account the normalization of the new $\mathbf{e}_r$ mode reduces the effect by a factor of the square root of the volume ratio. This leaves us with a residual increasing of μ that is approximately the square root of the repetition number M, reduced slightly by the weaker field at the waveguide edge. Conversely, the radiation efficiency of the bound surface plasmon does not appreciably change, a result of the scattering rate remaining constant when the number of apertures is increased without altering the density of apertures. Therefore, by repeating the structure laterally M times in a region where the waveguide modal field remains strong, we can increase τ_r/τ_e by a factor of approximately $\sqrt{M}$. As a result, by placing apertures laterally, the antenna inches closer to critical coupling (i.e., $\tau_e = \tau_r$). A comparison of 3-D FDTD simulations for one and three apertures depicted in Fig. 3. The emission of the three-aperture emitter is shown to exceed the one aperture emitter by ~1.6 which is close to the $\sqrt{3}$ ratio predicted by coupled mode theory. Still, since we excite the resonator from only one direction in the waveguide, and considering that μ and τ_e are given for coupling to both directions, the maximum possible emission is 50%

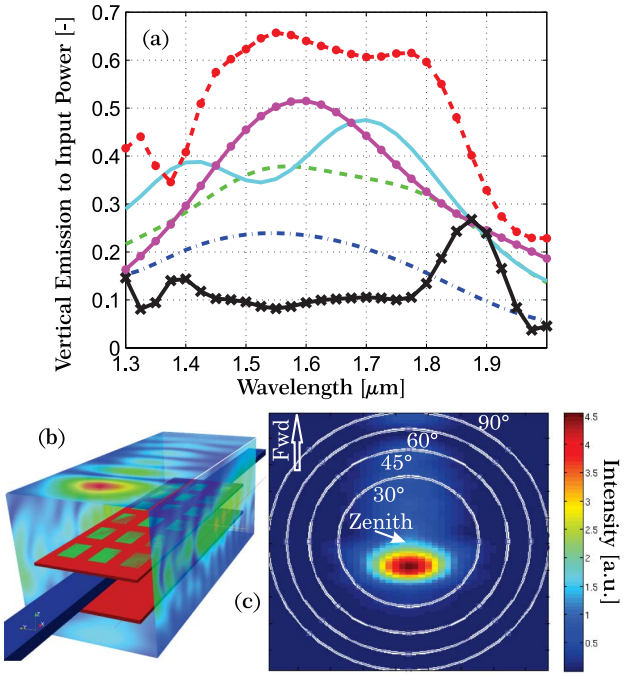

Fig. 3. (Color online) (a) Simulated vertical emission for structures with ground-plane: (blue dash-dotted) single aperture, (dashed green) three apertures arranged laterally to the waveguide direction, (solid cyan) 3×2 array design to emit exactly to zenith, (magenta solid-dots) 3×2 array design for 10° backward emission, (red dashed-line-dots) 3×6 array design for 5° backward emission and (black line-Xs) ohmic losses of 3×6 array. (b) The simulated 3×6 structure with the time integrated field box around it. (c) Far field pattern of the same structure at $\lambda = 1550$ nm.

in a symmetric structure. Higher efficiencies require excitations from both directions or non-symmetric emitters, a result that can be proven through reciprocity arguments.

In order to obtain the results in Fig. 3(a), we monitored the spectral content of the fields over the surface of a box enclosing the structure. From this, we calculated the amount of energy leaving each facet [Fig. 3(b)]. All other losses, including emission out of the sides, bottom, and rear of the structure had significantly lower values (ohmic losses are ~10% for the 6×3 antenna over most of the band and less for the smaller structures). In all cases depicted in Fig. 3, the structure includes a ground plane at a distance of $d \sim 3\lambda/4n$ for constructive vertical coupling. This was done to interfere the reflection of the bottom emission with the top emission and, thus, maximize the vertical coupling.

To further enhance the emission, the structure is repeated longitudinally in order to help couple the remaining field in the waveguide [see Fig. 1(c) and 3rd to 5th curves in Fig. 3(a)]. In this case, we can achieve greater than 50% coupling by breaking the symmetry of the problem and directing the emission to an angle from the surface normal which is half the way from the main lobe maximum to the first zero. This can be done by tuning the structure longitudinal period Λ to be slightly less than the bound resonant wavelength (0.9 μm instead of 1 μm). Curves 3 and 4 in Fig. 3(a) show this effect in the 3×2 apertures case, and the 5th curve shows 65% coupling using 3×6 apertures structure. Finally, looking at the far field pattern of the top facet emission [e.g., Fig. 3(c) for 3×6 case] shows that the main lobes in all structures has a 15° to 25° FWHM. The main lobe was centered at the zenith for the first 3 structures and at 10° and 5° back from the surface normal for the fourth and fifth structures, respectively.

Using 3-D FDTD simulations, we show that metallic nano-antenna structures can easily vertically couple 65% of an input bound wave with a structure only four free-space wavelengths in length. This structure is short and realistic, and uses commonly available materials. While compact all dielectric silicon emitters have been demonstrated [4], to our knowledge this is the first proposed and numerically verified compact emitter design in a Si_3N_4 waveguide, a relatively low index contrast system. By repeating the structure laterally and then longitudinally with a period, Λ, slightly shorter than the effective wavelength, highly efficient and extremely broadband emission is produced. We expect that in a silicon waveguide coupled to a nano-photonic antenna even greater efficiency would be possible due to the increased polarization current enabled by the high index contrast of a silicon waveguide.

This work is supported by the DARPA Microsystems Technology Office (MTO) under contract DE-AC04–94AL85000. We would like to thank Cheryl Sorace of MIT, Paul Davids and Rohan Kekatpure of Sandia, and Nader Engheta of University of Pennsylvania for helpful comments.

References

1. M. Fan, M. A. Popović, and F. X. Kärtner, in *OSA/CLEO* (2007), paper CTuDD3.
2. B. Wang, J. Jiang, and G. P. Nordin, Photon. Tech. Lett. **17**, 9 (2005).
3. K. Kintaka, Y. Kita, K. Shimizu, H. Matsuoka, S. Ura, and J. Nishii, Opt. Lett. **35**, 1989 (2010).
4. G. Roelkens, D. V. Thourhout, and R. Baets, Opt. Lett. **32**, 1495 (2007).
5. K. V. Acoleyen, H. Rogier, and R. Baets, Opt. Express **18**, 13655 (2010).
6. J. K. Doylend, M. J. R. Heck, J. T. Bovington, J. D. Peters, L. A. Coldren, and J. E. Bowers, Opt. Express **19**, 21595 (2011).
7. J. Li and N. Engheta, IEEE Aerospace Electron. Syst. Mag. **55**, 3018 (2007).
8. S. Scheerlinck, P. Dubruel, P. Bienstman, E. Schacht, D. V. Thourhout, and R. Baets, J. Lightwave Technol. **27**, 1415 (2009).
9. H. A. Haus, in *Waves and Fields in Optoelectronics*, N. Holonyak, Jr., ed. (Prentice-Hall, 1984), pp. 197–207.
10. B. E. Little, S. T. Chu, H. A. Haus, J. Foresi, and J. P. Laine, J. Lightwave Technol. **15**, 6 (1997).
11. H. A. Haus and W. P. Huang, IEEE Aerospace Electron. Syst. Mag. **79**, 1505 (1991).
12. H. R. Philipp, in *Handbook of Optical Constants of Solids*, E. D. Palik, ed. (Academic, 1998), pp. 760–774.